A highly efficient free-space fiber coupler with 45° tilted fiber grating to access remotely placed optical fiber sensor

SANKHYABRATA BANDYOPADHYAY[1], LI-YANG SHAO[1,2]*, WANG CHAO[3]**,
ZHIJUN YAN[4], FEI HONG[1], GUOQING WANG[1], JIAHAO JIANG[1], PING SHUM[1],
XIAOPING HONG[5], WEIZHI WANG[2]

[1]Department of Electrical and Electronic Engineering, Southern University of Science and Technology, Shenzhen, 518055, Guangdong, China
[2] Peng Cheng Laboratory, Shenzhen 518055, Guangdong, China
[3] School of Engineering and Digital Arts, University of Kent, Canterbury, CT2 7NT, U.K.
[4]School of Optical and Electronic Information, NGIA, Huazhong University of Science and Technology, Wuhan 430074, Hubei, China
[5]Department of System Design and Intelligent Manufacturing, Southern University of Science and Technology, Shenzhen, 518055, Guangdong, China
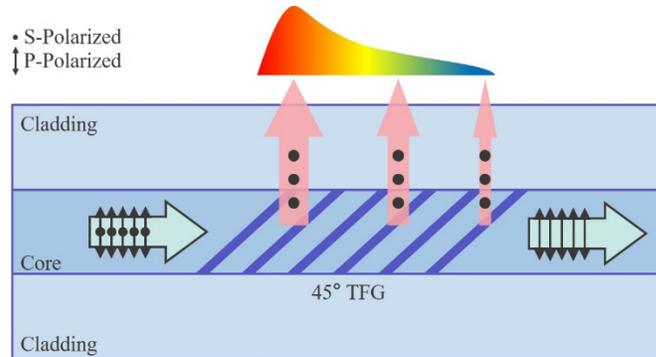* shaoly@sustech.edu.cn
** C.Wang@kent.ac.uk

Abstract: In this work, a 45° tilted fiber grating (TFG) is used as a waveguide coupler for the development of a portable interrogation system to access remotely placed optical fiber sensors. The TFG is directly connected to a remote fiber sensor and serves as a highly efficient light coupler between the portable interrogation unit and the sensor. Variation of strain and temperatures are measured with a standard fiber Bragg grating (FBG) sensor, which serves as a remotely placed optical sensor. A light beam from the interrogation unit is coupled into the TFG by a system of lenses, mirrors and optical collimator and acted as the input of the FBG. Reflected light from the FBG sensor is coupled back to the interrogation unit via the same TFG. The TFG is being used as a receiver and transmitter of light and constituent the key part of the system to connect "light source to the optical sensor" and "optical sensor to detector". A successful demonstration of the developed system for strain and temperature sensing applications have been presented and discussed. Signal to noise ratio of the reflected light from the sensors was greater than ~ 40 dB.

1. Introduction

Fiber-based components have made revolutionized progress in the application areas of a diverse field of engineering and instrumentation. Optical fibers-based components are considered to be a better choice for designing and fabrication of optical devices than bulk optical waveguides due to lower optical attenuation, ease of fabrication and lightweight. In particular, fiber Bragg grating (FBG) is a dominated sensor for the application of strain, temperature, pressure, accelerometer, and force sensing [1, 2]. It has also been widely used as highly sensitive sensors for biological applications [1-3]. In the case of FBG, forward propagating core mode is coupled with backward propagating core modes and a particular wavelength that satisfies the Bragg condition is reflected back to the input end [3]. Bragg wavelength (reflected light) is being governed by the effective index of the core mode and period of the grating structure [3]. In the case of tiled FBG (TFBG) with a slight tilt in the grating plane, the forward propagating core mode can be coupled to backward propagating cladding modes and higher-order radiation mode [1, 4]. It was demonstrated that with a higher index of modulation, the forward propagating core mode can be coupled effectively with higher-order symmetric cladding modes [5]. TFBG has been used in different fields of

applications due to inherent unique optical properties of TFBG. TFBG sensors are being widely used as chemical and biological sensors [1, 6-8], TFBG was also used for the detection of lateral force [9], 3D shape sensors [10] and force measurement applications [11]. A successful fiber optic viscometer was demonstrated with a superlattice modulated structure [12]. A tilted fiber grating (TFG) with a larger tilted angle between 23.1° and 66.9° to the perpendicular direction of the propagation plane of core mode can radiate the light out of fiber core with very strong polarization correlation [13]. A TFG has been used as in-line polarizer [14], in-fiber spectrometer [15], interrogator [16,17], fiber ring laser [18], In particular, a $45°$ TFG can tap 'S-polarized' light out from the fiber core while making the transmission part as 'P-polarized' light. $45°$ TFGs have been used as an efficient in-fiber polarizer [19-22] over the years. Very recently, a $45°$ TFG has been used successfully inline fiber diffraction grating with high efficiency for spectrally encoded imaging system [23], optical time stretching imaging [24], and full-duplex indoor optical communication [25].

In this work, it has been demonstrated for the first time that an FBG sensor can be accessed remotely (without direct connection to a source or detector via fiber) with the help of a $45°$ TFG, which is used as a highly efficient free-space coupler for reception and transmission of light. The signal from the FBG sensor can be read out clearly in an optical spectrum analyzer (OSA). Coupling strength of forward propagating and backward propagating core and cladding mode decreases rapidly with an enhancement of tilt angle of the plane of grating whereas the coupling of radiation mode with forward propagating core mode is being enhanced significantly. These radiation modes can be used as a source of free space light at a tilt angle near $\sim 45^0$. In this paper, it has been presented that with a system of plano-convex cylindrical and spherical lenses, mirrors and collimators, light can be guided from source to TFG and also efficiently in the reverse path. An FBG sensor is connected with the 45° TFG and the signal from FBG can be observed with a high signal to noise ratio (SNR) to the detector, which is not connected with FBG. The reflected light of FBG was coupled to a

remotely placed detector via
Fig. 1. Schematic diagram of coupling of polarization-dependent light to radiation mode in 45^0 TFG

the same TFG. The TFG is acting as receiver and transmitter of light simultaneously to connect the remotely placed FBG sensor to its light source and detector. As a demonstration of the concept, an FBG sensor was placed to measure the variation of temperature and strain as per the standard measurement principle of FBG [3, 26, 27]. The effective index of core mode gets changed with a change in temperature and strain as per thermo-optic and elasto optic coefficient of the glass the and as an immediate effect, a shift in the Bragg wavelength can be observed in the reflected spectrum [3, 27]. This FBG sensor will be accessed through a TFG fiber coupler and the signature of the FBG will be observed in the detector without direct connection of FBG to either with source and detector. This report shows proof of the principle of remotely access sensors by using 45° TFG as a waveguide coupler. In this paper, a narrow linewidth laser is being used as a source to access FBG sensor. In future, with

proper optimization of TFG coupler characteristics along with meticulously designed free-space optical components other optical sensors like long-period fiber grating [28], distributed Bragg reflector based laser sensors [29], fiber optic surface plasmon sensors [30], fiber interferometric sensors [31], LPFG sensors in reflection mode [32] can be accessed with the TFG coupler though the alignment process will be critical. This concept of remotely access sensors will be useful in many important engineering applications like an automated sensing platform where the light source needs to be connected occasionally with the optical sensors as per demand. This scheme of sensing is unique as it can access and characterize optical sensors irrespective of their packaging and working principles.

2. Operating Principle

A TFG with a tilt angle of 45^0 can tap the s-polarized light out of the fiber core and p-polarized light can be guided by the fiber. A 45^0 TFG was used successfully as an ideal inline fiber polarizer and integrated polarizer [13, 19-22]. Fig. 1 represents the schematic diagram of the working principle of 45^0 TFG, a detailed theoretical and experimental analysis of the radiation mode coupling was reported in earlier work [33,34]. The basic coupled-mode equations of the fiber Bragg grating are given as [4, 35]

$$\frac{dA^{co}}{dz} = ik_{01-01}^{co-co}A^{co} + i\frac{m}{2}k_{01-01}^{co-co}B^{co}\exp(-i2\delta_{01-01}^{co-co}z) + \sum_{v}i\frac{m}{2}k_{0v-01}^{cl-co}B_{ov}^{cl}\exp(-i2\delta_{0v-01}^{cl-co}z) \quad (1)$$

$$\frac{dB^{co}}{dz} = -ik_{01-01}^{co-co}B^{co} - i\frac{m}{2}k_{01-01}^{co-co}A^{co}\exp(-2i\delta_{01-01}^{co-co}z) \quad (2)$$

$$\sum_{v}\frac{dB_{0v}^{cl}}{dz} = -i\frac{m}{2}k_{0v-01}^{cl-co}A^{co}\exp(-i2\delta_{0v-01}^{cl-co}) \quad (3)$$

where A^{co} and B^{co} represents the amplitudes of forward and backward propagating core modes respectively. The term 'm' is induced modulation. $B_{0,v}^{cl}$ is the amplitude of the backward propagating cladding modes of the order v. k_{01-01}^{co-co} is the self-coupling coefficient between forward propagating core and backward propagating core mode. $k_{0,v-01}^{cl-co}$ are the cross-coupling coefficients between forward propagating core mode (LP_{01}) and backward propagating cladding modes (LP_{0v}). δ_{01-01}^{co-co} and δ_{0v-01}^{cl-co} are the detuning parameters.

The intensity of the radiation pattern of TFG can be expressed as [36]:

$$S = \frac{\pi c\varepsilon_0 n_0^2 \delta n^2 k_0^3 E_0^2}{4r}(\frac{\Delta^2}{k_0^2 n_0^2} + \frac{k_t^2}{k_0^2 n_0^2}\sin^2(\delta - \phi))F^2 \quad (4)$$

Where $F = \dfrac{K_s a J_0(ua)J_1(K_s a) - ua J_1(ua)J_0(K_s a)}{K_s^2 - u^2}$

where n_0 is the refractive index of the fiber core, δn is the modulated refractive index induced by ultraviolet light exposure, 'a' is the radius of fiber core, $k_0 = 2\pi/\lambda_0$ is the wave vector of the incident light, E_0 is the intensity of the electric field, β is the propagation constant, r is the radius of the fiber core, $\Delta = \beta - K_g$, $K_g = 2\pi cos\theta/\Lambda$, and $K_t = 2\pi sin\theta/\Lambda$ represent the longitudinal and transverse wavenumbers of the grating respectively, where Λ is the period of grating and θ is the tilted angle, $K_t = \sqrt{k_0^2 n_0^2 - (\beta - K_g)^2}$ is the projection of the wave vector of emergent light in transverse direction, δ and ϕ are the polarization and azimuthal angle of the radiated light, respectively, $K_s = \sqrt{k_t^2 + K_t^2 - 2k_t K_t \sin(\phi)}$ is the

mismatching among the wave vectors of grating, incident light, and emergent light, and u is the waveguide parameter of fiber and J is the Bessel function. A detailed volume current mode based theoretical study was accomplished recently followed by a detailed experimental study [29]. It was proved that the radiation mode of 45^0 TFG is highly polarized and the polarization-dependent suppression ratio can be as high as ~ 25 dB [13].

FBG sensor is being characterized by the developed system, FBG is being accessed with a source from a remote location. The reflected spectrum of FBG is governed by the Bragg reflection equation [3]

$$\lambda_{Bragg} = 2 * \Lambda * n_{eff}^{co} \tag{5}$$

Where Λ is the period of the grating and n_{eff}^{co} is the effective index of core mode. With a change in temperature and strain, the shift in Bragg wavelength is governed by the equation

$$\Delta\lambda_{Bragg} = 2 * \Lambda(\frac{\partial n_{eff}^{co}}{\partial T} + \frac{\partial n_{eff}^{co}}{\partial \varepsilon}) \tag{6}$$

Now with a change in temperature and strain, the effective index of the core mode varies as per the strain optic and thermo-optic coefficient of the fiber. The governing equation is as follows [3,26,27]:

$$\frac{\Delta\lambda_{Bragg}}{\lambda_{Bragg}} = (1 - p_e)\varepsilon \tag{7a}$$

$$\frac{\Delta\lambda_{Bragg}}{\lambda_{Bragg}} = 2[\Lambda \frac{\partial n_{eff}}{\partial T} + n_{eff} \frac{\partial \Lambda}{\partial T}] \tag{7b}$$

p_e is elasto optics coefficient and $\frac{\partial n_{eff}}{\partial T}$ is known as thermo optic coefficient of the glass materials. ∂T represents the variation in temperature and $\partial \varepsilon$ is the change of applied strain to the fiber.

3. Experiment and Discussion

FBG and 45° TFG are fabricated with standard inscription techniques. A 45° TFG was written into a Ge-doped typical telecom single-mode photosensitive fiber (SMF-28, Corning) using the standard scanning phase mask technique with continuous-wave UV laser light at 244 nm. The phase mask was rotated by 33.3° to achieve the required 45° slanted grating fringes in
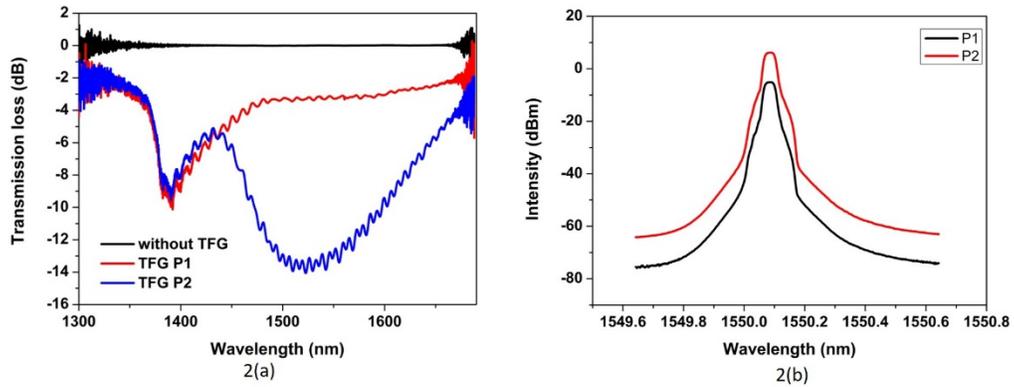

Fig. 2(a). The measured transmission spectrum of 45° TFG with SLED source, P1, P2-polarization states 1 and 2 respectively. Fig. 2(b). The measured power intensity of laser through TFG with two different states of polarization

the fiber core. The length of TFG was ~ 24 mm. The length of FBG ~ 20 mm. The central Bragg wavelength was ~ 1550 nm. In the beginning, to endure the amount of radiated light from the TFG, polarization-dependent loss (PDL) was measured with two distinct polarization states.

Received light by TFG
(Source-Col-Free space-TFG-OSA)

3(a)

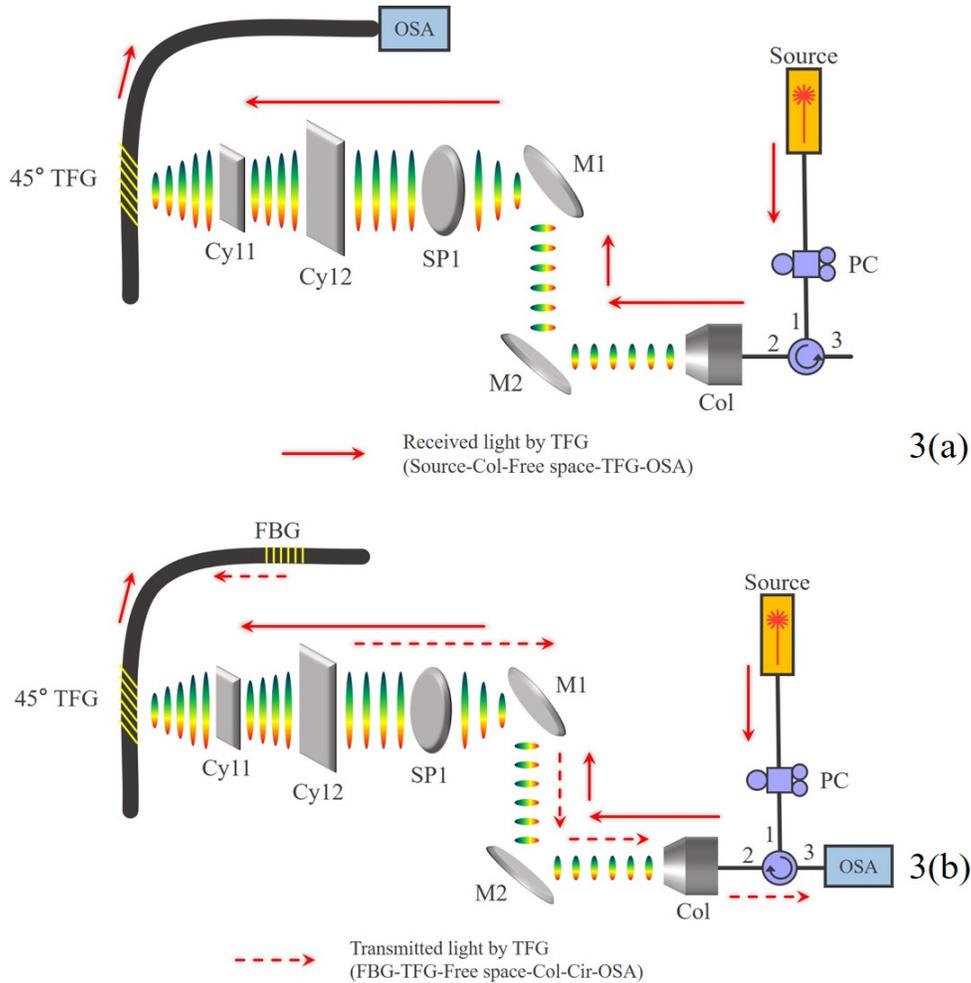Transmitted light by TFG
(FBG-TFG-Free space-Col-Cir-OSA)

3(b)

Fig. 3(a). Schematic bench-top diagram for measurement of received light by TFG. Fig. 3(b). Transmitted light by TFG initial alignment purpose, PC-polarization controller; Cyl1-Cylindrical lens 1, Cyl2-Cylindrical lens 2, SP1-Spherical lens 1, M1-Mirror 1, M2-Mirror 2, Col-Collimator, OSA-Optical Spectrum Analyzer.

Almost ~ 13 dB PDL has been found, PDL depends strongly on the length of the grating and modulation index of the core refractive index. It has been shown earlier that higher the modulation indexes the respective PDL is also more significant [19]. Fig. 2(a). shows the transmission spectrum of the TFG with SLED source (HOYATEK/HYSLED 1550), the SLED source is not polarized so a polarizer was used to achieve better performance. Fig. 2(b) shows the same with a laser source (Real photon/TSL-C). A strong polarization-dependent loss is being observed for both of the cases of the sources. The transmission loss spectrum of TFG shows a broadband loss spectrum near the C+L telecommunication band. That means quite a significant amount of light is being radiated out from the fiber. The optical alignment is the key part of the designing, in the beginning, the polarized light was launched into one end of TFG and coupled to the detector through lenses, mirrors, and collimator in a path

which can be defined as (TFG-free space-collimator). 'S' polarized light which is radiated out from the side face of the fiber core was successfully coupled to the detector through different arrangements of lens and mirrors. After successful alignment, for real-time measurement of the variation of strain and temperature with FBG sensor, the input light was launched in the port '1' of the circulator as is being shown in Fig. 3(a). The light emerges from the source and passes through a collimator (circulator port '2'), mirrors, and system of lenses and then reaches to the surface of TFG. The schematic representation of the experimental setup has been depicted in Fig. 3(a). The amount of received light in the distal end of TFG from the source was measured in OSA. The optical path can be defined as (Source-Collimator-Free space-TFG-OSA). A laser source is being used for the experiment. The recorded amount of light in OSA in the arrangement of Fig. 3(a) is being termed as 'received light' by TFG and is acting as an input for the FBG sensor for the rest of the experiments. In the following experiment, the FBG is connected with TFG, and laser light is launched as a source from circulator port '1'. The collimator is placed at port '2' of the circular and OSA is located at circular port '3' to measure the reflected light from FBG through lenses and mirrors after being radiated out from TFG. The schematic representation of the experimental set-up is being shown in Fig.3b. Reflected light from FBG can be detected in OSA (Fig. 3(b)) and it can be termed as 'transmitted light' through TFG. The light path is demarcated as (FBG-TFG-Free Space-Collimator-Circulator-OSA). The received and transmitted light of TFG was measured and it is shown in Fig. 4. the coupling loss from fiber to free space is near ~ 11 dB. It is to be noted that the radiated light from TFG is a highly
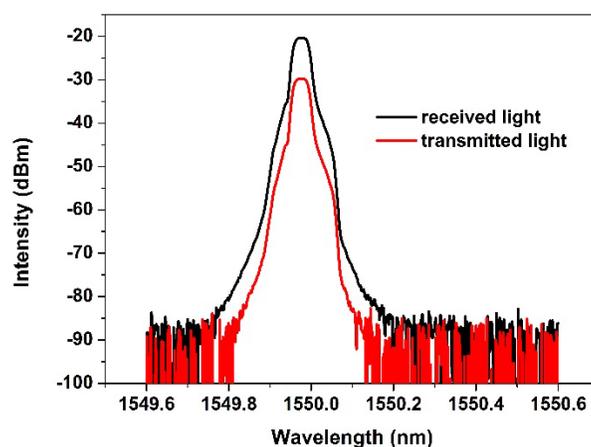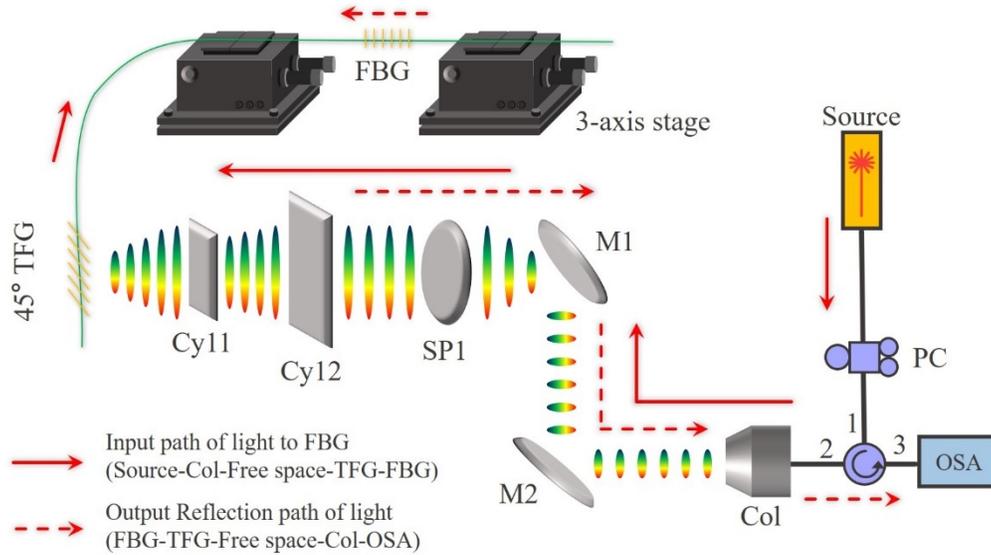

Fig.4. The measured spectrum in OSA with a) collimator-free space-TFG-OSA named as received light by TFG and FBG-TFG-free space-collimator-OSA (transmitted light).

diffracted beam in nature so the alignment needs to be done very accurately for successful reception of light in a detector. The TFG was mounted in fiber rotators (HFR007/Thorlabs) which are placed in two 3-axis stages (MAX312D /Thorlabs). The fiber is placed in a straight manner without any bend or stress and the rotators provide a degree of freedom for rotation. The TFG was rotated and placed over the 3-axis stage in such a way that the emergent beam is parallel to the optical table which was determined by the UV-laser card (VRC2/ Thorlabs) and visible IR alignment disk (VRC2D1/Thorlabs). A short focal length cylindrical lens (LJ1874L2C, Plano-convex cylindrical lens/focal length ~ 7.7 mm/ Thorlabs) was used for the collimation purpose after ensuring the horizontal emergent of the beam from TFG surface through fiber rotators the radiation beam is highly divergent. The cylindrical lens (LJ1328L2/C, plano-convex cylindrical lens/ focal length ~ 20 mm) was used after the short focal cylindrical lens to reduce the diffraction further. A plano-convex spherical lens (LA1951C, focal length ~ 25.4 mm) was used to focus the cylindrical beam on a spherical spot of light to the mirror. A telescopic mirror arrangement (BB1-E04/Thor labs, broadband

dielectric mirror, 1280 nm-1600 nm) is employed before the collimator which seems to be very useful for efficient alignment of light between the lens and collimator. Mirrors were mounted on (KM100/Thor labs) mirror clamp which can provide two effective additional

degrees of freedom for the alignment purpose. It is to be mentioned that the quality of collimator is also played an important role in alignment, the best alignment was observed with (F230 APC Collimator/ focal length was ~ 4.61 mm and NA ~ 0.54). The output light of the collimator was measured in an

Fig. 5. The schematic diagram for the experimental set-up to access FBG with TFG.

optical spectrum analyzer (OSA, YOKOGAWA/AQ6370D) which is placed at port '3' of the circulator. The response of FBG was characterized by a change in temperature and strain. FBG was placed in a temperature bath and the temperature was changed in a step of 10 degrees from room temperature and the reflected output from FBG was detected in OSA.
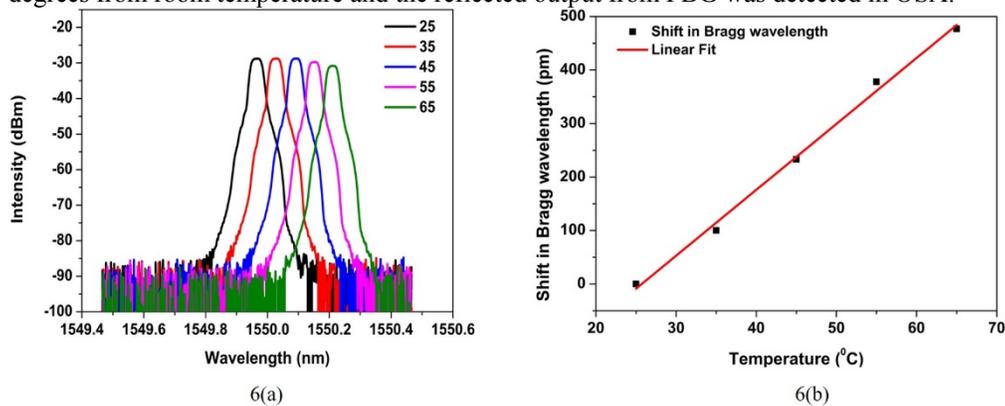

6(a)

6(b)

Fig. 6(a). The recorded spectrum of FBG at five different temperatures 25^0 C, 35^0 C, 45^0 C, 55^0 C, and 65^0 C, respectively Fig. 6(b). Measured Bragg wavelength shift with the variation of temperature.

In the case of reflection, the light follows the path (FBG-TFG-Free Space Arrangements-Collimator-Circulator-OSA) and the spectrum was recorded in OSA. The temperature of the bath was measured with a standard thermocouple for a proper reference. It has been ensured that there is no additional loading or bending over the FBG during the entire time of temperature measurement. The recorded spectrum of FBG for different temperatures is being shown in Fig. 6(a), the shift in resonance Bragg wavelength with the change in temperature is given in Fig. 6(b). The temperature sensitivity of the FBG was found to be ~ 11 pm/degree centigrade change in temperature which is similar to the other reported literature work [3]. In the case of measurement of strain, two 3- axis stages (MAX312D /Thorlabs) were used to produce some change in the tensile strain of FBG as mentioned in other reported work [37].

The applied change in strain has been found from the very basic definition of ($\Delta \varepsilon = \dfrac{\Delta l}{l}$).

The applied strain was varied from 0 to 400 µε, and the measured Bragg reflected spectrum with different applied strain has been depicted in Fig. 7(a). The recorded shift of the Bragg wavelength with a change in applied strain is shown in Fig. 7(b). The shift is ~ 1.3pm/ change in µε which is also quite similar to the previously measured value of strain sensitivity of FBG. In this paper, we demonstrate that the TFG can act as successful waveguide coupler for launching and reception purpose of light simultaneously to measure the wavelength shift of the reflected light from a remotely placed sensors which is not directly connected to any source or detector. As proof of the concept experiment, the total length of the free-space optical path was ~ 1.75 meters (including an intermediate distance of fibers, lenses, mirrors, and collimator). The coupling loss between free space to fiber and vice-versa path is almost ~ 11 dB.
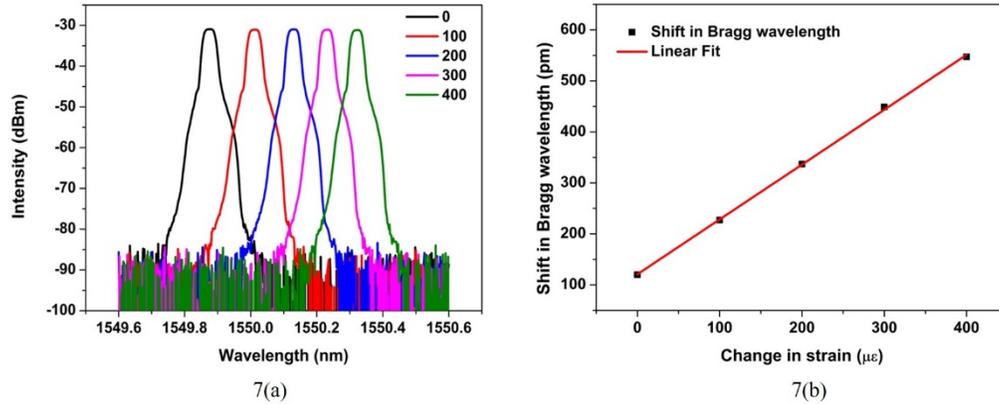

7(a)　　　　　　　　　　　　　　　　7(b)

Fig. 7(a). The measured spectrum of FBG based sensors during a change of strain, 0 µε, 100 µε, 200 µε, 300 µε, and 400 µε, respectively Fig.7(b). measured Bragg wavelength shift of FBG for different values of tensile strain

4. Conclusion

In this work, an initial experimental setup towards the development of a portable system to access remotely placed optical sensors is being demonstrated. 45° tilted fiber grating is being used as a waveguide coupler to characterize an FBG sensor for strain and temperature measurement. This research is a step towards the development of a hand-holding portable system to characterize any optical sensors as this TFG fiber coupler can be packaged easily with any optical sensors, (optical sensors + TFG coupler) can be work as a unit. The concept of portable sensors characterization systems will be helpful in the case of structural health monitoring, aeronautical engineering, and biomedical instrumentation. It will reduce the effort and cost of maintenance of the system. An automated platform can be developed where the software can select a particular sensor for the inspection purpose. In this report, we have

shown that an FBG can be characterized without direct connection neither with the source nor with the detector. The response of FBG with a change in physical parameters is analyzed with OSA and a narrow linewidth laser source is employed for the experiment. It has been understood the characteristics of TFG in terms of polarization-dependent loss and insertion loss are important to assess the domain of the light source for the system. A large and broad PDL spectrum of TFG is required for an applications where broadband source (BBS) will be used. In practice, we need to use BBS in different applications so the characteristics of TFG are very crucial. This TFG coupler may extend its application in sensors like long-period fiber grating, fiber laser sensors, fiber SPR sensors and fiber interferometric based application. In future work, the photodiode will be used to make the system more compact and portable. The SNR of the measurand signal is quite high and is around ~ 40 dB. It has been apparent that the properties and position of the lenses and mirrors play the most crucial role in the case of alignment. A distinct set of lenses is being used for proper alignment but the process of alignment is not easy. Properties of TFG can be tailored to achieve the best coupling performance from free space to the fiber sensor. Besides, the parameters of the collimator also need to be chosen critically as per the designing aim and scope of the applications. Collimator with a higher numerical aperture (NA) can be useful for more coupling of light from free space to fiber. The coupling efficiency of TFG can be improved further by using a rod lens and an oil-immersion objective lens, which can be studied in future work. In the future, commercial modules can be developed as a handheld system for the characterization of optical sensors for different engineering applications.

Acknowledgment

Disclosure
The authors declare that there are no conflicts of interest related to this article.

References

1. J. Albert, L.-Y. Shao, C. Caucheteur, "Tilted Fiber Bragg grating Sensors," Laser Photonics Rev., 7, 83-108 (2013).
2. C. Broadway, R. Min, A. G. L. Junior, C. Marques, and C. Caucheteur "Toward Commercial Polymer Fiber Bragg Grating Sensors: Review and Applications" IEEE J. Lightwave Technol. 37 (11), 1605-2615 (2019).
3. A. Othonos, and K. Kalli, Fiber Bragg gratings. Artech House, Boston, MA, (1999).
4. T. Erdogan and J. Sipe, "Tilted fiber phase gratings," J. Opt. Soc. Am. A., vol. 13, no. 2, pp. 296-313, 1996.
5. S. Bandyopadhyay, T. Dey, N. Basumallick, P. Biswas, K. Dasgupta, and S. Bandyopadhyay "High Sensitive Refractometric Sensor Using Symmetric Cladding Modes of an FBG Operating at Mode Transition" IEEE J. Lightwave Technol. 34 (14), 3348-3353 (2016).
6. C. Caucheteur, T. Guo, F. Liu, B.-Ou Guan, and J. Albert "Ultrasensitive plasmonic sensing in air using optical fibre spectral combs" Nat. Commun., 7, 13371 (2016).
7. J. Lao, P. Sun, F. Liu, X. Zhang, C. Zhao, W. Mai, T. Guo, G. Xiao, and J. Albert, "In situ plasmonic optical fiber detection of the state of charge of supercapacitors for renewable energy storage. " Light: Sci. Appl., 7(1) 34-41 (2018).
8. Z. Liu, C. Shen, Y. Xiao, J. Gong, J. Wang, T. Lang, C. Zhao, C. Huang, Y. Jin, and X. Dong, "Liquid surface tension and refractive index sensor based on a tilted fiber Bragg grating," J. Opt. Soc. Am. B., 35(6), 1282-1287 (2018).
9. L.-Y. Shao and J. Albert, "Lateral force sensor based on a core-offset tilted fiber Bragg grating," Opt. Commn, 284 (7), 1855-1858, (2011).
10. D. Feng, W. Zhou, X. Qiao and J. Albert "Compact Optical Fiber 3D Shape Sensor Based on a Pair of Orthogonal Tilted Fiber Bragg Gratings" Scientific Reports | 5:17415 | DOI: 10.1038/srep17415, 2015
11. C. Shen, C. Zhong, D. Liu, X. Lian, J. Zheng, J. Wang, Y. Semenova, G. Farrell, J. Albert, and J. F. Donegan, "Measurements of milli-Newton surface tension forces with tilted fiber Bragg gratings," Opt. Lett., 43(2), 255-258 (2018).

12. H. Qian, L.-Y. Shao, W. Zhang, X. Zhang, H. He, B. Luo, X. Zou, W. Pan, and L. Yan, "Fiber-optic viscometer with all-fiber acousto-optic superlattice modulated structure", IEEE J. Lightwave Technol., 36(18), 4123-4128 (2018).

13. Z. Yan, C. Mou, K. Zhou, X. Chen, and L. Zhang" UV-Inscription, Polarization-Dependant Loss Characteristics and Applications of 45° Tilted Fiber Gratings" IEEE J. Lightwave Technol., 29(18), 2715-2724 (2011).

14. P. S. Westbrook, T. A. Strasser, and T. Erdogan, "In-line polarimeter using blazed fiber gratings," IEEE Photon. Technol. Lett., 12(10), 1352-1354 (2000).

15. S. Remund, A. Bossen, X. Chen, L. Wang, A, Adebayo, L. Zhang, B. Povazay, and C. Meier "Cost-effective optical coherence tomography spectrometer based on a tilted fiber Bragg grating" SPIE BiOS, 2014, San Francisco, California, United States, 2014.

16. P. Cheben, E. Post, S. Janz, J. Albert, A. Laronche, J. H. Schmid, D. X. Xu, B. Lamontagne, J. Lapointe, A. Delage, and A. Densmore "Tilted fiber Bragg grating sensor interrogation system using a high-resolution silicon-on-insulator arrayed waveguide grating" Opt. lett., 15(22), 2647-2650 (2008).

17. T. Gang, F. Liu, M. Hu, and J. Albert "Integrated Differential Area Method for Variable Sensitivity Interrogation of Tilted Fiber Bragg Grating Sensors" IEEE J. Lightwave Technol. 37 (18), 4531-4536 (2019).

18. B. Lu, C. Zou, Q. Huang, Z. Yan, Z. Xing, M. A. Araimi, A. Rozhin, and C. Mou "Widely Wavelength-Tunable Mode-Locked Fiber Laser Based on a 45°-Tilted Fiber Grating and Polarization Maintaining Fiber" IEEE J. Lightwave Technol. 37 (14), 3571-3578 (2019).

19. K. Zhou, G. Simpson, X. Chen, L. Zhang, and I. Bennion "High extinction ratio in-fiber polarizers based on 45° tilted fiber Bragg gratings" Opt. Lett. 30(11), 1285-1287 (2005).

20. G. Bharathan, D. D. Hudson, R. I. Woodward, S. D. Jackson, and A. Fuerbach, "In-fiber polarizer based on a 45-degree tilted fluoride fiber Bragg grating for mid-infrared fiber laser technology," OSA Continuum, 1(1), 56-63 (2018).

21. M. T. Posner, N. Podoliak, D. H. Smith, P. L. Mennea, P. Horak, C. B. Gawith, P. G. Smith, and J. C. Gates, "Integrated polarizer based on 45° tilted gratings," Opt. Express., 27 (8), 11174-11181 (2019).

22. Q. He, Z. Xing, X. Guo, Z. Yan, Q. Sun, C. Wang, K. Zhou, D. Liu, and L. Zhang "In-fiber single-polarization diffraction grating based on radiant tilted fiber grating," Opt. Lett., 44(17), 4407-4410 (2019).

23. G. Wang, C. Wang, Z. Yan, and L. Zhang, "Highly efficient spectrally encoded imaging using a 45° tilted fiber grating," Opt. Lett., 41(11), 2398-2401 (2016).

24. G. Wang, Z. Yan, L. Yang, L. Zhang, and C. Wang "Improved Resolution Optical Time Stretch Imaging Based on High Efficiency In-Fiber Diffraction" Scientific Reports (2018) 8:600 |DOI:10.1038/s41598-017-18920-8.

25. G. Wang, U. Habib, Z. Yan, N. J. Gomes, Q. Sui, J. Wang, L. Zhang, and C. Wang, "Highly efficient optical beam steering using an in-fiber diffraction grating for full duplex indoor optical wireless communication," IEEE J. Lightwave Technol. 36 (19), 4618-4625 (2018).

26. L. Xu, N. Liu, J. Ge, X. Wang, and M. P. Fok "Stretchable fiber-Bragg-grating-based sensor" Op. lett. 43(11), 2503-2506 (2018).

27. W. C. Du, X. M. Tao, and H. Y. Tam "Fiber Bragg Grating Cavity Sensor for Simultaneous Measurement of Strain and Temperature" IEEE Photonic Tech L, 11(1), 105-107, (1999).

28. S. Bandyopadhyay, L. Y. Shao, M. Smietana, J. Hu, C. Wang, Q. Wu, G. Q. Gu, Y. J. Liu, X. L. Chen, Z. Q. Song, X. F. Song, and Q. L. Bao, "Study on optimization of nano-coatings for ultra-sensitive biosensors based on long-period fiber grating", Sensing and BioSensing Research 27: 100320, (2020).

29. X. Yang, S. Bandyopadhyay, L.-Y. Shao, D. Xiao, G. Gu, and Z. Song, "Side-Polished DBR Fiber Laser with Enhanced Sensitivity for Axial Force and Refractive Index Measurement", IEEE Photonics J. 11(3),1-10, (2019).

30. X. Zhang, X. S. Zhu, Y. W. Shi "Fiber optic surface plasmon resonance sensor based on silver-coated large-core suspended-core fiber" Opt. Lett. 44(18), 4550-4553, (2019).

31. M. S. C. Velazquez, L M. L-Marin, and J H Cordero" Fiber optic interferometric immunosensor based on polydimethilsiloxane (PDMS) and bioactive lipids" Biomed. Opt. Express., 11(3), 1316-1326, (2020).

32. F. Esposito, A. Zotti, R. Ranjan, S. Zuppolini, A. Borriello, S. Campopiano, M. Zarrelli, and A. Iadicicco "Single-Ended Long Period Fiber Grating Coated With Polystyrene Thin Film for Butane Gas Sensing" IEEE J. Light. Technol., 36(3), 825-831 (2018).

33. Y. Lu, W. Huang, and S. Jian, "Full vector complex coupled mode theory for tilted fiber gratings," Opt. Express, 18(2), 713-726 (2010).

34. H. Qin, Q. He, Z. Xing, X. Guo, Z. Yan, Q. Sun, K. Zhou, H. Wang, D. Liu and L. Zhang" Numerical and Experimental Characterization of Radiation Mode of 45° Tilted Fiber Grating" IEEE J. Light. Technol., 37(15), 3777-3783 (2019).

35. T. Erdogan and J. E. Sipe. "Radiation-mode coupling loss in tilted fiber phase gratings." Opt. Lett. 20(18), 1838-1840 (1995).

36. Y. Li, M. Froggatt, and T. Erdogan, "Volume current method for analysis of tilted fiber gratings," IEEE J. Light. Technol., 19(10), 1580-1591(2001).

37. K. Tian, G. Farrell, X. Wang, W. Yang, Y. Xin, H. Liang, E. Lewis, and P. Wang, "Strain sensor based on gourd-shaped single mode-multi mode-single-mode hybrid optical fibre structure", Opt. Express, 25(16), 18885-18896 (2017).